The Astrophysical Journal Letters, 755:L27 (5pp), 2012 August 20 doi:10.1088/2041-8205/755/2/L27

DETECTION OF LOW-VELOCITY COLLISIONS IN SATURN'S F RING

N. O. Attree, C. D. Murray, N. J. Cooper, and G. A. Williams
Queen Mary University of London, Astronomy Unit, Mile End Road, London E1 4NS, UK; N.O.Attree@qmul.ac.uk
Received 2012 April 21; accepted 2012 July 18; published 2012 August 2

ABSTRACT

Jets of material extending several hundred kilometers from Saturn's F ring are thought to be caused by collisions at speeds of several tens of ms^{-1} between ∼10 km diameter objects such as S/2004 S 6 and the core of the ring. The subsequent effects of Keplerian shear give rise to the multi-stranded nature of the F ring. Observations of the ring by the Imaging Science Subsystem experiment on the *Cassini* spacecraft have provided evidence that some smaller protrusions from the ring's core are the result of low-velocity collisions with nearby objects. We refer to these protrusions as "mini-jets" and one such feature has been observed for ∼7.5 hr as its length changed from ∼75 km to ∼250 km while it simultaneously appeared to collapse into the core. Orbit determinations suggest that such mini-jets consist of ring material displaced by a ∼1 ms^{-1} collision with a nearby moonlet, resulting in paths relative to the core that are due to a combination of Keplerian shear and epicyclic motion. Detections of mini-jets in the *Cassini* images suggest that it may now be possible to understand most small-scale F ring structure as the result of such collisions. A study of these mini-jets will therefore put constraints on the properties of the colliding population as well as improve our understanding of low-velocity collisions between icy objects.

Key words: planets and satellites: dynamical evolution and stability – planets and satellites: rings

1. BACKGROUND

Saturn's F ring, located 3500 km outside the main ring system, contains a variety of structures with scales ranging from ∼1 to ∼200 km that change on timescales ranging from hours to years (Porco et al. 2005; French et al. 2012). Features include the regular "streamer-channel" phenomenon caused by the gravitational influence of the two nearby shepherding moons Prometheus and Pandora (Murray et al. 2005). Also seen are "jets" of material which evolve through Keplerian shear from initially near-radial, linear features to form the spiral strands which lie on either side of the core (Charnoz et al. 2005; Murray et al. 2008). Jets are created by physical collisions between the core and ∼5 km radius moonlets, such as S/2004 S 6, which inhabit the F ring region (Murray et al. 2008; Charnoz 2009; see, e.g., Figure 1 of Murray et al. 2008). The material is spread over hundreds of kilometers in semi-major axis implying an impact with the core at relative velocities of ∼30 ms^{-1} (Charnoz et al. 2005; Murray et al. 2008).

S/2004 S 6 is now thought to be one member of a population of bodies with a range of sizes and orbits which interact with the ring (Murray et al. 2008). Perhaps the first evidence for such a population came from the depletion of magnetospheric charged particles measured by Pioneer 11 and interpreted as due to a 2000 km wide belt of 0.1–10 km moonlets (Cuzzi & Burns 1988). Direct imaging by the *Hubble Space Telescope* during the edge-on viewing geometry in 1995/1996 showed large (∼10 km) extended objects spread across the whole region (McGhee et al. 2001) but these were not seen by *Voyager* nor indeed by *Cassini* to date. Stellar occultations by the *Cassini* UVIS and VIMS instruments revealed 15 semi-transparent "clumps" and two opaque moonlets, with sizes from 10 s of meters to ∼1 km laying within the ring or strands (Esposito et al. 2008; Meinke et al. 2012), while data from the *Cassini* Imaging Science Subsystem (ISS) experiment led to the discovery of S/2004 S 6 as well as numerous small (∼1 km), shadow-casting objects close to the ring (Beurle et al. 2010). Numerical simulations of streamer channels show that regions of high particle density and low relative velocity can form (Beurle et al. 2010), raising the possibility of Prometheus-induced clumping of material as a formation mechanism for this local population (see also Esposito et al. 2012). Other theoretical work, e.g., Canup & Esposito (1995) and Karjalainen (2007), has explored tidally modified accretion, relevant at the F ring's orbital radius, which produces a bimodal particle size distribution with a number of large bodies among the small ring particles. Charnoz et al. (2010) suggest that a population of moonlets at the F ring is a natural product of ring spreading and gravitational instability. Together this suggests a ring surrounded by a population of objects, with a range of sizes, orbits, and strengths, which would be expected to interact with it, gravitationally and through collisions.

Changes in brightness have indeed been explained as dust released by collisions, with previous work suggesting either the embedded population (Barbara & Esposito 2002; French et al. 2012) or interplanetary meteoroids (Showalter 1998) as the primary cause. The ring remains irregular and changeable down to smaller scales, displaying "kinks," "clumps," and other features (Porco et al. 2005). In particular, some features appear morphologically very similar to the jets described above (compare Figure 1 of Murray et al. (2008) with Figure 1) but on radial scales that are much smaller (∼50 km) and have therefore been termed mini-jets. These are observed throughout the F ring but interpreting their origin has previously been difficult as they are usually only seen in perhaps 2–4 consecutive images. The rest of this paper describes observations of mini-jets, in general, and in one case where the time evolution of a feature has been detected.

2. OBSERVATIONS

For the purposes of identification, we define mini-jets to be small-scale (typically ∼40–180 km in radial extent and $\ll 1^\circ$ in longitude) features appearing to emanate from the core of the F ring. This excludes kinks and bright clumps which lie entirely within the core, but includes a variety of morphologies, as seen

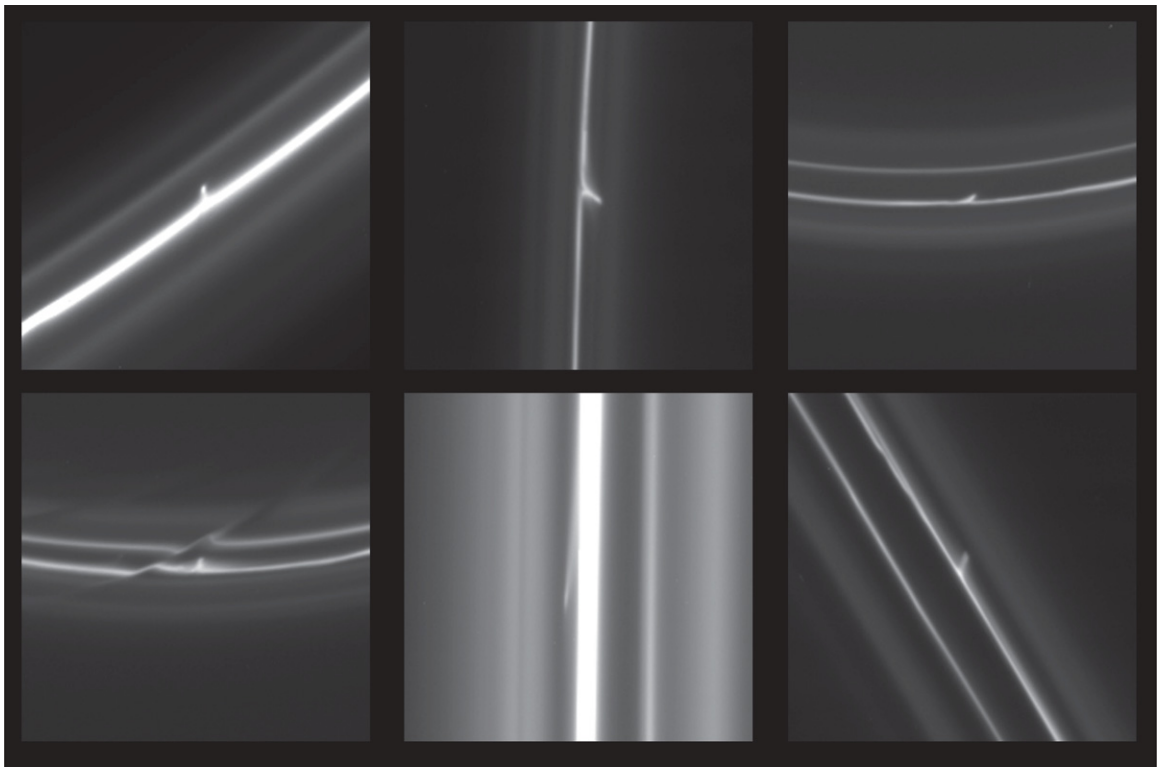

Figure 1. Examples of mini-jets detected in *Cassini* ISS Narrow Angle Camera (NAC) images. The image numbers and dates are from left, top: N1501710723 (2005 August 2), N1542050711 (2006 November 12), and N1578411831 (2008 January 7), bottom: N1578427113 (2008 January 7), N1589117591 (2008 May 10), and N1597907705 (2008 August 20). The corresponding approximate lengths are 29, 136, 155, 43, 129, and 32 km.

in Figure 1. These range from classic small jets to longitudinally extended objects near the ring or at the boundary of the bright dust sheet surrounding it. A search of all *Cassini* ISS sequences containing resolved images of the F ring has been performed to produce a catalog of ∼570 mini-jet features with an average of ∼10 visible in the ring at any one time. Most are only observed in one or two images over the course of ∼10 minutes and are not seen again. A few examples have been caught at opposite ansa, i.e., approximately half an orbital period later, but one notable mini-jet has been identified in a sequence of images lasting ∼7.5 hr (see Figure 2). It was observed for an extended period because it happened to fall within the coverage of a streamer-channel observation, ISS_102RF_FRSTRCHAN001_PRIME, designed to track Prometheus and its perturbation around the ring over a full orbit. The mini-jet appears in 138 images, each separated by ∼4 minutes, meaning it is visible for approximately half of an F ring orbital period.

The left-hand side of Figure 3 shows three frames from a movie of the image sequence, cropped and re-projected in an equal-aspect radius/longitude system. The mini-jet appears as a trail at an angle from the vertical (i.e., radially outward direction) which increases with time while its tip moves radially inward toward the ring.

Measurements of the mini-jet's position over time allow an orbit to be fitted. Fits for the orbital elements (semi-major axis, a, eccentricity, e, inclination, I, longitude of ascending node, Ω, and longitude of periapse, ϖ) for the tip of the mini-jet, an object next to it, and the F ring core at the time of observation are presented in Table 1. The F ring core orbit was derived from a geometric fit of an inclined, precessing, elliptical ring to measured positions of the bright core, covering one orbit, from the same ISS image sequence used to measure the jet. Unlike

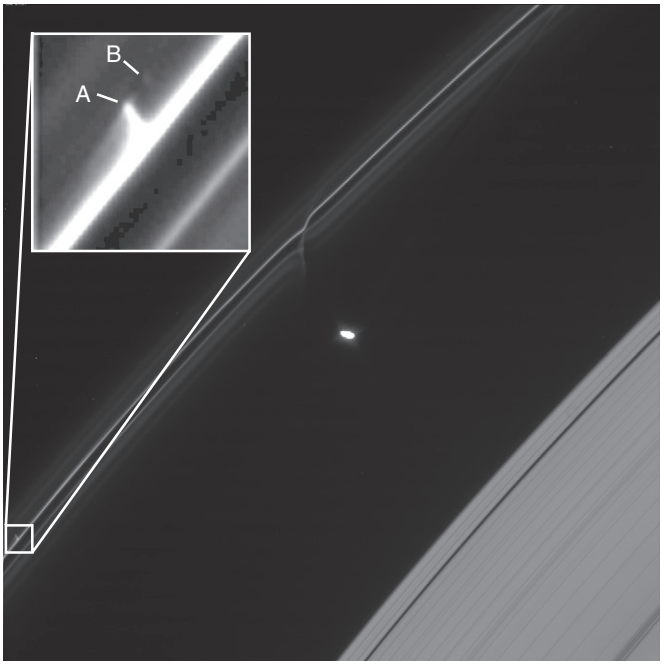

Figure 2. *Cassini* image N1612002457, taken on 2009 January 30, at 09:47:26 with a 1.5 s exposure and showing ∼6° of ring. A ∼50 km mini-jet is highlighted and enhanced in the inset. The jet tip (A) has a faint but traceable object (B) trailing it as well as the faint "spray" of material which connects the leading (left) side of the jet to the F ring core. This is the first in a sequence of 138 images, each separated by ∼4 minutes, which capture the evolution of this feature.

previously published orbit models for the F ring core, which are averaged over several years, it therefore represents a precise local snapshot of the core orbit in the vicinity of the jet during

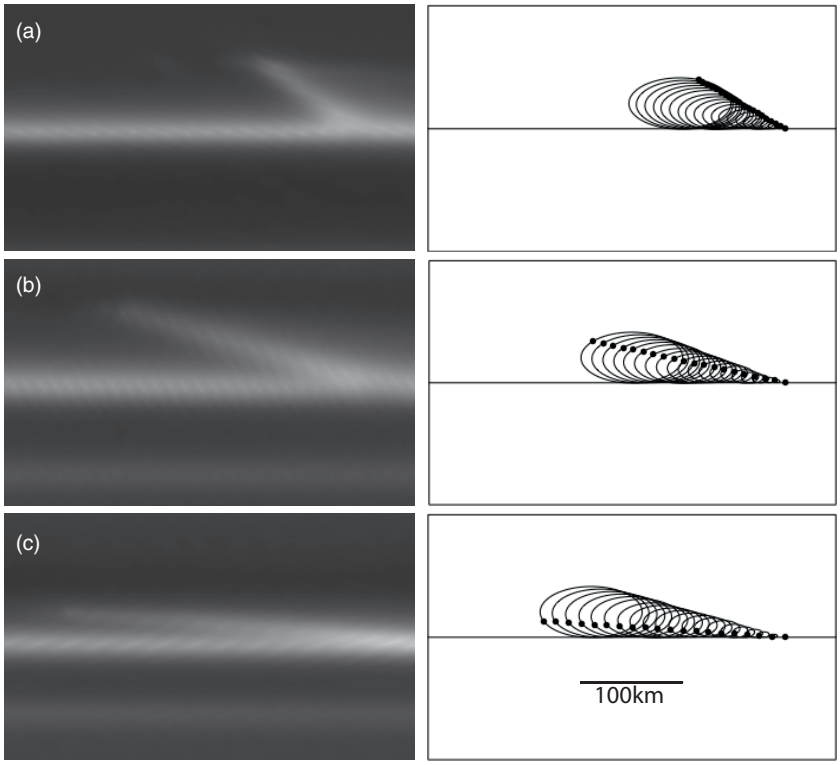

Figure 3. Left: reprojected ISS NAC images separated by ~3 hr. Images are (a) N1612002457, (b) N1612013501, and (c) N1612022286. Right: corresponding frames from an animation of particles (denoted by filled black circles), displaced from the ring by a range of Δa and Δe, undergoing relative orbital motion. The particles follow epicyclic paths around the ellipses with centers that drift downstream (to the left) at a constant rate due to Keplerian shear. The reprojected images and the animation are to the same scale and each covers 400 × 220 km.

Table 1
Orbital Elements for the F Ring Core, Mini-jet Tip, and Mini-jet Object at the Epoch 2009 January 30 09:45:00:00

	a (km)	e	I (°)	Ω (°)	ϖ (°)
F-ring Core	140215.1 ± 0.2	$0.0023108 \pm 8 \times 10^{-7}$	0.0063 ± 0.0001	102.3 ± 0.7	341.98 ± 0.02
Mini-jet Tip	140242 ± 4	$0.00251 \pm 3 \times 10^{-5}$	0.005 ± 0.001	70 ± 10	340.9 ± 0.5
Mini-jet Object	140246 ± 8	$0.00251 \pm 5 \times 10^{-5}$	0.004 ± 0.002	86 ± 9	340.8 ± 0.7

its formation and evolution. Table 1 shows that the tip of the mini-jet is displaced from the core by 27 ± 4 km in semi-major axis and $1.992 \pm 0.3 \times 10^{-4}$ in eccentricity (uncertainties are derived from the tip measurement errors which dominate) with the rest of the jet material having similar but smaller offsets.

The evolution of the feature with respect to the F ring core as shown in Figure 3 can now be understood as a combination of Keplerian shear and epicyclic motion. Objects on moderately eccentric orbits can be thought of as traveling on centered ellipses of semi-axes, ae and $2ae$, around a guiding center which itself follows a circular path around the primary (Murray & Dermott 1999). The mini-jet is composed of a number of particles each displaced from the F ring by a range of Δa, Δe which will each follow their own centered ellipse relative to the ring. At the same time, the Δa offset leads to Keplerian shear of the guiding centers of each ellipse at a rate of $\Delta\lambda/\Delta t = (-3/2)(n/a)\Delta a$, where $\Delta\lambda$ is the offset after a time Δt for an orbit with mean motion n. The combined effects lead to the motion of the jet radially inward toward the ring while it simultaneously lengthens downstream in longitude. This can be seen in a simple model animation, frames from which are shown to the right of the re-projected images in Figure 3. Extrapolating this motion backward to the point where all the particles lie in the ring at the same location suggests the mini-jet formed from an instantaneous impulse ~6.57 hr before the first observation.

Toward the end of the movie the mini-jet re-enters the ring and becomes difficult to resolve. In theory it should begin to re-emerge on its second cycle as the particles follow their epicycles away from periapse and radially outward toward apoapse again. However, it is possible that the mini-jet may not survive re-collision with the F ring core. In our example the issue is complicated by the presence of Prometheus which, purely by chance, reaches its closest approach near the longitude of the mini-jet and could have perturbed it gravitationally. The relevant section of corotating longitude has been examined in the preceding and succeeding sets of observations and no definitive detection of a re-merging mini-jet has been made.

ISS has obtained 10 streamer-channel movies to date, representing 27.°99 days of coverage (time and longitude coverage are both important for observing over significant portions of an orbit). With only one mini-jet event observed, this is a frequency, ν, of 0.036 per degree per day or ~13 in the entire ring per day. The number observed at any one time in the ring should be $N = \nu\tau$ on average, where τ is the average lifetime. In addition, mini-jets will only be visible when radially extended outward or inward from the core, which, for these epicycles,

is the case for 70%–80% of a cycle for $\Delta a = 27$–50 km size jets and a 10 km thick core, respectively. Taking a lifetime of $\sim$1 cycle = 0.6196 days our crude, resolution-dependent calculation suggests $\sim$8 mini-jets should be visible in the F ring at any one time, comparable with the estimate derived from other types of observation.

3. COLLISIONAL DYNAMICS

We now investigate the physical mechanisms that can result in a $\sim$27 km change in a ring particle's semi-major axis on a timescale of hours or less. The evolving mini-jet is clearly not associated directly with the Prometheus perturbation, being located upstream from it, while other large bodies capable of such gravitational interactions were not detected and in any case would produce features with positive *and* negative values of Δa (Beurle et al. 2010). However, physical collisions *are* able to create similar, and even larger, features (Charnoz 2009). We therefore investigate the dynamics of such collisions to put constraints on potential impactors.

Assuming a near instantaneous collision, transferring a velocity impulse $\Delta\mathbf{v}$, we can rewrite the standard perturbation equations (see, e.g., Chap. 2 of Murray & Dermott 1999) as

$$\Delta a = \frac{2}{n\sqrt{1-e^2}}\left[e\Delta v_R \sin f + \Delta v_T(1 + e\cos f)\right] \quad (1)$$

$$\Delta e = \frac{\sqrt{1-e^2}}{na}\left[\Delta v_R \sin f + \Delta v_T(\cos f + \cos E)\right], \quad (2)$$

where Δa and Δe are the instantaneous changes in the elements of an orbit with parameters as before, at a true anomaly f and eccentric anomaly E, due to radial and transverse impulses Δv_R and Δv_T, respectively.

Using the F ring orbit from Table 1, with f and E at the inferred time of collision, with values of Δa and Δe from above and solving Equations (1) and (2) simultaneously gives

$$\Delta v_T = 1.6 \pm 0.2 \text{ ms}^{-1}, \qquad \Delta v_R = -1.1 \pm 1.7 \text{ ms}^{-1}$$

for the maximum impulses. Errors have been estimated using the uncertainties in Δa and Δe quoted above. The rest of the particles which make up the jet receive smaller impulses, between this and zero, but with approximately the same ratio between the components (approximately the same orientation of the total $\Delta\mathbf{v}$), although the specific orientation and position of each particle may vary and is clearly less sensitive to the radial component. This change in velocity of the ring particles, resulting from the collision, unfortunately does not lead directly to the velocity vector of the collider, which remains unknown (and with multiple possible answers). However, some elementary dynamics permits constraints to be placed on the collision.

Moving to a particle-centered frame the pre- and post-impact relative velocities can be resolved into components normal (subscript n) to, and tangential (subscript t) to, the point of collision. These are related to one another via the corresponding coefficients of restitution, ϵ_n and ϵ_t, by

$$\mathbf{u}' = \epsilon_n \mathbf{u}_n + \epsilon_t \mathbf{u}_t,$$

where $\mathbf{u}$ denotes a relative velocity, $\mathbf{u} = \mathbf{v}_{\rm imp} - \mathbf{v}_{\rm part}$ is the difference in velocity between the impactor and the F ring particle, and primed symbols indicate post-impact quantities. Coefficients of restitution vary with impact velocity, composition, temperature, etc., but are likely to be low (i.e., highly dissipative) for icy particles, especially if coated with a frosty regolith. Bridges et al. (1984) and Charnoz (2009) have the coefficients decreasing with velocity and $\epsilon_n \sim 0.1$ for low ($\sim$1 ms^{-1}) impact speeds.

$\Delta\mathbf{v}$ for the F ring particle can be related to the relative impact velocity from conservation of linear and angular momentum by (Equation (14) of Richardson 1994)

$$\Delta\mathbf{v} = \mathbf{v}' - \mathbf{v} = \frac{m_{\rm imp}}{M}\left[(1+\epsilon_n)\mathbf{u}_n + \beta(1-\epsilon_t)\mathbf{u}_t\right], \quad (3)$$

where $M = m_{\rm imp} + m_{\rm part}$ is the total mass of the impactor and the F ring particle and the other parameters are as before with the addition of β, a dimensionless quantity between 0 and 1, related to the moments of inertia of the two particles. As in Charnoz (2009) this can be set to unity for highly dissipative collisions, ignoring particle spin.

For a moonlet–dust-particle collision $m_{\rm imp} \gg m_{\rm part}$ and $m_{\rm imp}/M \to 1$. If we treat the normal and tangential components symmetrically, assuming $\epsilon_n \approx \epsilon_t \approx \epsilon$, then Equation (3) is simplified to

$$\Delta\mathbf{v} \approx \mathbf{u} + \epsilon(\mathbf{u_n} - \mathbf{u_t}) \sim \mathbf{u}. \quad (4)$$

Hence the velocity impulse given to our dust particle is approximately equal to the relative velocity between the F ring and the colliding object plus a small factor which is dependent on the specific geometry of the collision. Thus for dissipative collisions, dust particles should be placed on similar orbits to the colliding bodies, as in Charnoz (2009). This may explain why nearby objects often seem to define the edge of the F ring dust envelope as described above.

Assuming this scenario the impacting object must have an orbit close to that of the ring and similar to that of the jet itself. The lack of a negative Δa feature on the other side of the core, as seen in some simulations (Charnoz 2009), constrains the geometry of the impact to those not generating any opposite transverse impulse. The relative velocity of the tip object at the time of collision fits these constraints ($\mathbf{u} \sim \Delta\mathbf{v}$), assuming a favorable distribution of material in the ring, making it a good candidate for the colliding body and, if this mini-jet is typical, for one of a population of such nearby objects.

4. THE LOCAL POPULATION

In the absence of rapid damping, we expect a population of objects originating in the F ring but gravitationally perturbed by Prometheus, as suggested by Beurle et al. (2010), to be spread around the ring with a range of orbital parameters up to a maximum of $\Delta a = \pm 19$ km, $\Delta e = \pm 13 \times 10^{-5}$, and $\Delta\bar{\omega} = \pm 4^\circ$ (Murray et al. 2008), with the relative eccentricity (incorporating the differences in eccentricities and longitudes of periapse between the two bodies) $\Delta e_r \approx \Delta a/a$ for these objects (Williams 2009). This means that they will return to the ring, or thereabouts, roughly once per orbit near their periapses or apoapses, possibly colliding and creating a mini-jet each time. The largest relative radial and transverse velocities at these points of intersection can be calculated and are found to be $u_R \approx \pm 3.5$ ms^{-1} and $u_T \approx \pm 1.5$ ms^{-1}, which is consistent with jets of roughly the observed scale.

The fact that $\Delta a \approx a\Delta e_r$ for the colliding objects is important because it restricts the relative orientations of the intersecting orbits. If this symmetry is broken, for example, by unconstrained differential precession due to Saturn's non-spherical gravity terms, we would expect to find differences in the longitudes of

periapsis from 0° to 180°. Allowing this range for the colliders in the above calculations leads to large relative radial velocities ($\sim$75 ms^{-1}) and, from Equation (2), large radial impulses and therefore mini-jet eccentricities resulting in excursions from the F ring of hundreds of kilometers. S/2004 S 6 does produce jets on the $\sim$200 km scale but mainly through the effect of Δa rather than Δe. Instead what is seen is symmetry in the mini-jet orbital elements (as would be expected for a purely transverse impulse) so that they should always return to near the core after one cycle. It also implies that the colliders do not often cross the ring, remaining on one side and creating mini-jets which also stay on the same side of the ring.

The most likely explanation for this lack of highly eccentric mini-jets from anti-aligned colliders is that nearby objects are not freely precessing, suggestive of a core with significant mass holding the orbits in relatively close alignment.

If the $\sim$13 mini-jets estimated per day are each from one object that collides, on average, once an orbit then at least $\sim$8 such objects are required. If only a fraction of collisions produces an appreciable mini-jet, because of a clumpy, irregular core, then the total number of impacting objects could be much larger. For example, we could estimate this fraction to be the average area of aggregates like those in Esposito et al. (2008) (1.5×10^3 to 1.4×10^4 objects of average radius $\sim$450 m) over the total cross-sectional area of the F ring ($2\pi a_{\rm F} H$ with semi-major axis $a_{\rm F}$ and height H), i.e., assuming mini-jets are only created in collisions with dense core clumps. In this case, we would require $\sim$7000 colliding bodies for the observed number of mini-jets. We believe that jets and mini-jets represent the outcome of two ends of a continuum of objects that collide with the F ring, the evolution of all being dominated by Keplerian shear.

5. CONCLUSIONS

We have investigated the phenomenon of mini-jets—small-scale, irregular features in Saturn's F ring. *Cassini* observations have shown the time evolution of a mini-jet to be a combination of Keplerian shear and epicyclic motion resulting from an initial displacement in semi-major axis and eccentricity. This displacement is consistent with the impulse from a collision with a small (<1 km) object on a nearby orbit, itself probably displaced by Prometheus.

If, as it now appears, this is typical of all $\sim$570 cataloged mini-jets it is now possible to understand most small-scale F ring features as the result of such collisions, reinforcing the notion of Murray et al. (2008) that the ring is shaped by a local moonlet swarm in addition to the gravitational effect of Prometheus (Murray et al. 2005; Beurle et al. 2010). The objects producing the mini-jets represent one end of a continuum with objects such as S/2004 S 6 at the other extreme.

Future work, to include detailed modeling and a more in-depth statistical analysis, will seek to confirm this and put constraints on the size, distribution, and orbits of the colliding bodies as well as helping to improve our understanding of low-velocity collisions between icy objects.

We are grateful to Phil Nicholson for his comments on an earlier draft of this paper and to the UK Science and Technology Facilities Council for their financial support.

Facility: Cassini

REFERENCES

Barbara, J. M., & Esposito, L. W. 2002, Icarus, 160, 161
Beurle, K., Murray, C. D., Williams, G. A., et al. 2010, ApJ, 718, L176
Bridges, F. G., Hatzes, A., & Lin, D. 1984, Nature, 309, 333
Canup, R. M., & Esposito, L. W. 1995, Icarus, 113, 331
Charnoz, S. 2009, Icarus, 201, 191
Charnoz, S., Porco, C. C., Déau, E., et al. 2005, Science, 310, 1300
Charnoz, S., Salmon, J., & Crida, A. 2010, Nature, 465, 752
Cuzzi, J. N., & Burns, J. A. 1988, Icarus, 74, 284
Esposito, L. W., Albers, N., Meinke, B. K., et al. 2012, Icarus, 217, 103
Esposito, L. W., Meinke, B. K., Colwell, J. E., Nicholson, P. D., & Hedman, M. M. 2008, Icarus, 194, 278
French, R. S., Showalter, M. R., Sfair, R., et al. 2012, Icarus, 219, 181
Karjalainen, R. 2007, Icarus, 189, 523
McGhee, C. A., Nicholson, P. D., French, R. G., & Hall, K. J. 2001, Icarus, 152, 282
Meinke, B. K., Esposito, L. W., Albers, N., & Sremcevic, M. 2012, Icarus, 218, 545
Murray, C. D., Beurle, K., Cooper, N. J., et al. 2008, Nature, 453, 739
Murray, C. D., Chavez, C., Beurle, K., et al. 2005, Nature, 437, 1326
Murray, C. D., & Dermott, S. F. 1999, Solar System Dynamics (Cambridge: Cambridge Univ. Press), 158
Porco, C. C., Baker, E., Barbara, J., et al. 2005, Science, 307, 1226
Richardson, D. C. 1994, MNRAS, 269, 493
Showalter, M. R. 1998, Science, 282, 1099
Williams, G. A. 2009, PhD thesis, Queen Mary Univ. London